

# Printed sensor and liquid actuation on natural fiber based substrate

J. J. Saarinen\*, P. Ihalainen, A. Määttänen, R. Bollström and J. Peltonen

Center for Functional Materials, Laboratory of Paper Coating and Converting,  
Åbo Akademi University, Porthansgatan 3, FI-20500 Åbo/Turku, Finland

\*jarkko.j.saarinen@abo.fi

## ABSTRACT

We demonstrate two new printed functionalities on a recently developed natural fiber based substrate. First, all-printed UV-A light detector is obtained using conductive polyaniline polymer, which changes its resistivity under UV-A irradiation. Secondly, electric field assisted wetting is realized using printed silver electrodes. Detailed topographical characterization of the porous, permeable, and rough fiber substrate is performed, which is crucial for optimizing electric functionality of such devices. Printed functionality on a natural fiber based substrate is expected to provide a more sustainable approach for applications such as sensors and displays that are currently printed on plastic films.

**Keywords:** printed functionality, inkjet, roughness, sensing, wetting

## 1 INTRODUCTION

Printed functionality and intelligence is a quickly growing market with forecasts of up to 300 billion US dollars by 2025 – a figure that is comparable to the size of the current silicon-based industry [1]. The key advantage of a roll-to-roll printing process is efficiency as large areas (i.e. large number of devices) can be produced with very low unit cost. Thus, cost-efficient radio-frequency identification (RFID) devices are already finding applications in monitoring logistics [2], and they may even replace barcodes in packages in future.

Recently natural fiber based substrates have found applications outside of the conventional graphical arts industry. For example, thin, lightweight, and foldable thermochromic displays have been realized on a regular copy paper [3] where thermochromic ink was utilized with patterned electrodes on the other side of the paper. Such devices can be used as extremely low cost displays (less than 0.10 US \$/m<sup>2</sup> [3]) suitable for data reporting on portable point-of-care devices. This is important especially in developing countries where laboratories and clean room facilities are not available for diagnostics. Bioactive paper is also a promising candidate for inexpensive sensing without any need for instrumentation [4]. Typically biological sensing applications require good control of wetting properties as

most biological substances are detected on wet phase. Therefore it is important to control surface and wetting properties of paper to obtain a good printing result and good performance e.g. in biosensing.

Conventionally this is managed by treating the paper surface with sizing agents that lower surface energy, increase advancing water contact angle (CA), and reduce water penetration into paper. However, a specific coating structure is needed to control the roughness and barrier properties of paper for functional printing as shown by Bollström *et al.* [5] who demonstrated an all-printed transistor functionality on such a substrate. For sensing purposes a growing interest has been pointed towards controlled wetting by external stimulus i.e. how CA can *dynamically* be varied and how wetting can either be improved or inhibited by an external driving force. The approach has been two-fold: on the one hand, one can modify surface to be stimuli responsive being sensitive to the environment or to externally applied impetus such as pH, light, X-rays, solvent, or temperature. On the other hand, external electric field can be employed to modify liquid drops and films providing fast, accurate, and reproducible changes in surface wetting. The external electric field induces spreading of electrically conductive liquid droplets, which can be used for liquid actuation in microfluidic devices and lab-on-a-chip applications. Such an approach has also found applications in optofluidics, for example, in microlenses, fiber optics, and liquid displays; for detailed description see a review by Mugele and Baret [6].

Here we demonstrate two applications of printed functionality on a newly developed natural fiber based substrate [5]. For good electrical conductivity a multilayer coating process is needed to smooth the rough fiber substrate and surface topography is investigated in detail using atomic force microscopy (AFM). Indeed, good electrical conductivity can be realized with a sufficient number of prints using a conductive silver ink. Here inkjet printed conductive polymers are used to demonstrate that UV-A sensitive sensor functionality can be realized. We also demonstrate how the external electric field can be applied to modulate wetting of liquids. To the best of our knowledge, this is the first time when electric field assisted wetting is demonstrated on a natural fiber based substrate.

## 2 EXPERIMENTAL

Paper substrate was in-house developed multilayer coated fiber based substrate suitable for printed functionality [5]. Precoated basepaper was first blade coated with a kaolin layer to smooth the surface. A barrier layer of styrene acrylic copolymer latex in a blend with precipitated calcium carbonate (PCC) was coated on top of the smoothing layer. Thin and smooth top layer provides well-controlled sorption properties via controlled thickness and porosity for good printability. Kaolin blended with 12 pph of styrene-butadiene latex was coated by reverse gravure coating (Mini-Labo, Yasui Seiki Co., USA). Only recyclable constituents were used for paper substrate to maintain recyclability. The structure of the developed substrate is shown in Fig. 1.

Silver electrodes were flexographically printed using an IGT GST2 laboratory scale printability tester with commercial OHKAFLEX<sup>®</sup> (Shore A 64° – 66°) photopolymer plates. The anilox cylinder had a cell angle of 45° with 40 lines/cm and a volume of 20 ml/m<sup>2</sup>. The printing speed was set to 0.5 m/s. The pressure between the anilox cylinder and the plate as well as the pressure between the plate and the substrate was set to 50 N. All prints were performed at 23.0 ± 0.2 °C room temperature (RT) and 50 ± 2 % relative humidity (RH). Commercial silver ink diluted in methyl ethyl ketone (MEK, 50 wt%) was supplied by Creative Materials and designed for pad printing. The original ink was further diluted by adding MEK with a 5:1 weight ratio of ink to MEK.

Polyaniline (PANI, emeraldine salt, 6.3 wt % dispersion in toluene) was purchased from Panipol Ltd. (Finland). The emeraldine oxidation non-conductive stage can be converted to a conducting polymer with the protonic acid doping process. The printing ink was a mixture of PANI: o-dichlorobenzene (o-DCB) with a ratio of 1:2. The ink was filtered with 0.2 μm polypropylene (PP) filter before printing with a laboratory scale piezoelectric inkjet printer Dimatix DMP-2800 (Fujifilm

Dimatix Inc., Santa Clara, USA). Single nozzle with a voltage of 17 V with 10 pl and 10 μm drop volume and spacing, respectively, were applied on drop-on-demand mode. The printing was performed at 22.0 ± 2 °C RT and 22.0 ± 3 % RH.

The printed Ag electrodes were cured using infrared (IR) drier (IRT systems, Hedson Technologies AB, Sweden) consisting of three lamps and a fan. Heating temperature and time of the substrate was approximately 180 °C and 5–10 s, respectively.

Square resistance of the printed conducting silver was measured using a Keithley Multimeter (Keithley Instruments Inc., Cleveland, USA) with a measured area of 8 × 10 mm<sup>2</sup>. The UV-lamp used in the PANI UV-A response measurements was a Bluepoint 4 ecocure (Dr. Hönle AG, Germany) used with a UV-A filter having a maximum intensity of 2000 mW/cm<sup>2</sup> at the wavelength of 365 nm.

Atomic force microscopy (AFM) analysis was performed with a NTEGRA Prima scanning probe microscope (NT-MDT, Russia) in intermittent contact mode. The microscope was placed on an active vibration isolation table (TS-150, Table Stable Ltd., Germany), which was further placed on a concrete stage to eliminate external vibrational noise. Topographical imaging was carried out using coated rectangular tips (NSC15 / AIBS, MikroMash). All images (1024 × 1024 pixels) were measured in ambient conditions (RH = 30 ± 2 %, RT = 23 ± 1 °C). The free amplitude of an oscillating cantilever was 55–60 nm. Damping ratio (contact amplitude / free amplitude) of approximately 0.5 and scanning frequency of 0.2 Hz were used for imaging.

The contact angle measurements were performed with a commercial contact angle goniometer KSV CAM 200 (KSV Instruments Ltd., Finland). The images were captured by a digital CCD camera and analyzed using the KSV CAM software with a standard deviation of approximately ± 3°. The CAs of purified water (Millipore) and cationic polydimethyldiallylammonium chloride (polyDADMAC) (Ciba®Alcofix®169, Ciba Specialty Chemicals) solutions on Ag prints were measured in ambient conditions (RT 23 ± 1 °C, RH 30 ± 5%).

## 3 RESULTS

Figures 2 a–c show typical AFM topographic images of a) coated paper substrate, b) flexographic print after the first Ag layer, and c) Ag layer after four successive prints. The AFM image of the coated paper substrate resolves plate-like kaolin pigments mixed with latex binder (Fig. 2a), which is a typical feature of such coatings. After printing with diluted Ag ink solution the surface is composed of plate-like Ag particles (Figs. 2b and 2c) resting on a topographically featureless film. Although the form of Ag particles is rather irregular, average diameter of 8 μm and height of 1 μm for an indi-

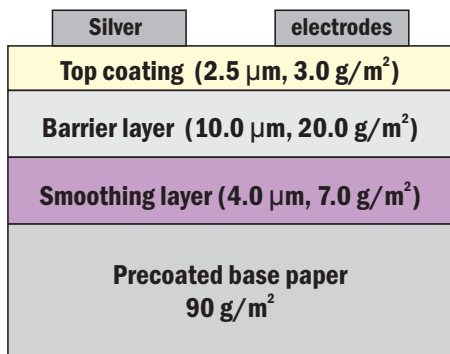


Figure 1: Natural fiber based substrate structure with coating thicknesses and grammages.

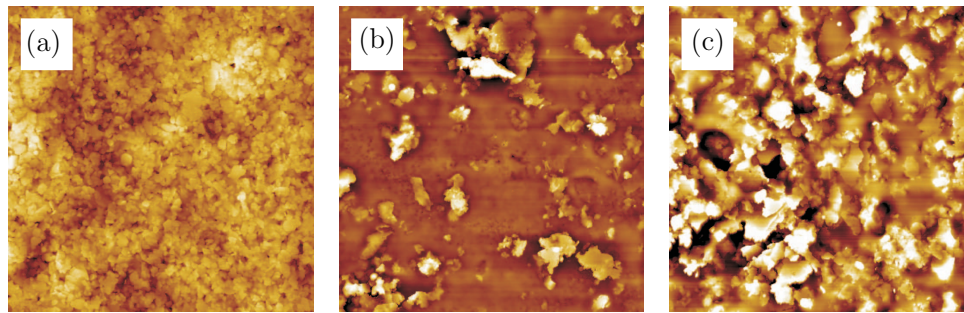


Figure 2: A typical AFM topographical images of the surface of the paper substrate (a) before printing, (b) after the first Ag print, and (c) after four successive Ag prints. The image size for (a) is  $20 \times 20 \mu\text{m}$ , and for (b) and (c)  $100 \times 100 \mu\text{m}$ . The height scale is 300 nm for (a), 1000 nm for (b) and (c).

vidual plate-like particle can be estimated. Flocculation of Ag particles is evident as some of the particulates at the surface are significantly larger than the aforementioned dimensions. The relative surface coverage of Ag particles increased after each successive printing reaching a coverage of approximately 50 % after the fourth print.

The square resistance is dramatically dropped after the fourth print to a value less than  $1 \Omega/\square$  from the level of  $G\Omega/\square$  for the first three prints. This is caused by the formation of a continuous conductive path after exceeding the silver threshold coverage value. The four successive prints are also needed with the reference poly(ethylene phthalate) (PET) plastic film to obtain conductivity. Recently we have achieved conductive electrodes with only a single flexographic print using an anilox roller with higher number of lines/cm resulting in a better surface coverage of Ag particles. Naturally we could use inkjet printing also for the Ag electrodes having smaller dimensions than possible with flexographic printing. However, the current electrode dimensions allow utilization of faster and more cost-efficient flexographic printing. IR sintering (oven sintering for plastic film) is required for good conductivity that is achieved with 4 successive prints both on the natural fiber based substrate and on plastic film.

Conductive polymers have raised immense interest within the past decades after their original discovery by MacDiarmid, Shirakawa, Heeger *et al.* in 1977 [7] as they provide mechanically flexible and transparent electrodes e.g. for organic light emitting diodes (OLEDs), polymer LEDs, and solar cell applications (for an excellent review, see Nobel lecture by Heeger [8]). Recently Lin *et al.* [9] showed that UV irradiation is followed by a reduction of the work function and conductivity of spin-coated PANI on glass surface. Here we study the UV-A response of inkjet printed PANI on paper substrate and the results are shown in Fig. 3. The temperature effects do not play role in the response as external heating did

not change the resistivity. We observe that UV-A irradiation lowers the resistance. However, here the process parameters are different compared by Lin *et al.* [9] that may explain the alternative response to the UV-A irradiation as resistance is decreased. We observe very stable and reproducible changes in resistivity that can be utilized as a simple UV-A irradiation detector.

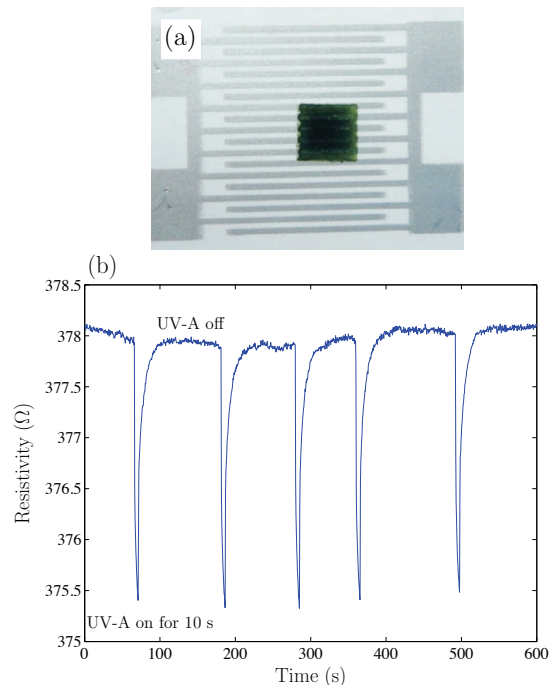


Figure 3: (a) A photograph of the inkjet printed PANI appearing as a dark square on the Ag finger electrodes. The dimensions of the device are as follows: the line width for the Ag-lines is  $400 \mu\text{m}$  with a spacing of  $400 \mu\text{m}$ , the width of the finger channel 15 mm, and PANI region  $4.5 \times 4.5 \text{ mm}^2$ . (b) Resistance is lowered when the polymer is exposed to the UV-A irradiation as seen from the resistance curvature as a function on time.

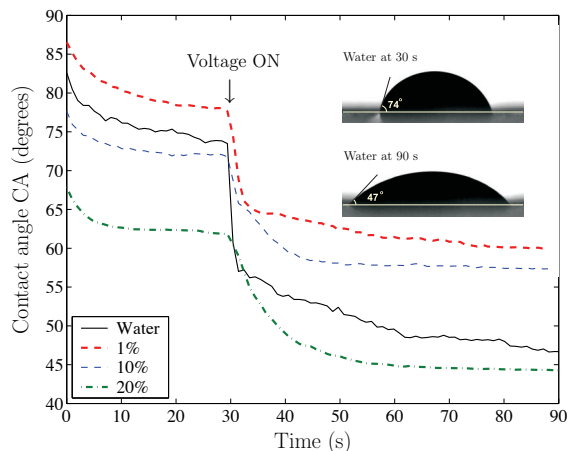


Figure 4: CA of water and polyDADMAC solutions as a function of time. The step like function in the CA is caused by voltage triggering at 30 s. The insert displays water droplet images before and after triggering.

Possibility to control surface wetting is attractive for various industrial applications such as coatings, functional printing, and paint industry. Adjusting the surface hydrophilicity or hydrophobicity has been widely investigated ranging from completely non-wetting superhydrophobic “Lotus-leaf” surfaces to completely wetting superhydrophilic surfaces, both in natural [10] and artificially structured [11] materials. Wetting in these structures is a *static* parameter as the physical structure and chemical properties of the surface define the static CAs. Thus, the CA measurement can be used to study surfaces in basic materials research.

Figure 4 shows the measured CAs for water and three different (1%, 10%, and 20%) polyDADMAC solutions averaged from three measurements. Small absorption occurs into the top coating layer, which is stabilized to equilibrium at 30 s. All CA measurements were performed on different spots on the paper substrate. Triggering the external electric potential of 20 V at 30 s immediately influences droplet spreading and CAs are lowered as shown in Fig. 4. The fastest and largest change in the CA is observed with pure deionized water having a conductivity of  $91 \times 10^{-6}$  S/m. The measured conductivity and viscosity of 100 % polyDADMAC solution were 2.63 S/m and 1.05 Pa·s with a shear rate of 1.93 1/s, respectively. Adding polyDADMAC into deionized water increases both conductivity and viscosity of the droplet. However, the higher viscosity dominates the response as seen in Fig. 4, i.e. the spreading of a droplet due to the external potential becomes slower with increasing amount of polyDADMAC as more work is required to overcome the increased viscosity.

The highest initial CA is observed with 1 % polyDADMAC solution. However, the difference in the initial CAs between water and polyDADMAC solution of 1

% is within the standard deviation whereas 20 % polyDADMAC solution clearly shows that polyDADMAC in higher dosages acts as a surfactant lowering the initial CA. The fastest and largest change is observed with pure deionized water with the smallest viscosity. The observed change in wetting induced by electric potential is irreversible due to porous top coating layer.

## 4 CONCLUSIONS

We have demonstrated here that the newly developed natural fiber based substrate [5] is suitable for functional printing and manufacturing of simple sensor templates. A key for good performance in printing electronics on paper is the control of surface topography that has been examined in detail by AFM. Smooth top coating layer allows development of simple printed functional devices such as UV-A irradiation detector. Furthermore, external electric field can be applied to improve wetting of liquids on paper substrate and spreading of functional coatings and inks on paper.

It is believed that paper substrates will find many applications in printed functionality in future as paper is one of the most abundant renewable materials available. Suitability for roll-to-roll process flow allows significant reduction in the unit cost of the printed functional devices and leads towards a more sustainable future with recyclable constituents.

## Acknowledgments

The Academy of Finland (grant no 118 650) and Stiftelsen för Åbo Akademi forskningsinstitut (travel grant) are acknowledged for financial support.

## REFERENCES

- [1] R. Das and P. Harrop, IDTechEx report, 7, (2008).
- [2] R. Bansai, IEEE Antennas Propag. Mag., 45, 105–106, (2003).
- [3] A. C. Siegel, S. T. Phillips, B. J. Wiley, and G. M. Whitesides, Lab Chip, 9, 2775–2781, (2009).
- [4] R. Pelton, Trends Anal. Chem., 28, 925–942, (2009).
- [5] R. Bollström *et al.* Org. Electron., 10, 1020–1023, (2009).
- [6] F. Mugele and J.-C. Baret, J. Phys.: Condens. Matter, 17, R705–R774, (2005).
- [7] C. K. Chiang *et al.*, Phys. Rev. Lett., 73, 1098–1101, (1977).
- [8] A. J. Heeger, Rev. Mod. Phys., 73, 681–700, (2001).
- [9] Y.-J. Lin, F.-M. Yang, C.-S. Lin, J. Appl. Phys., 102, 103702, (2007).
- [10] W. Barthlott and C. Neinhuis, Planta, 202, 1–8, (1997).
- [11] G. McHale, Nature Mater., 6, 627–628, (2007).